This is the accepted manuscript made available via CHORUS. The article has been published as:

Geometry of random potentials: Induction of two-dimensional gravity in quantum Hall plateau transitions

Riccardo Conti, Hrant Topchyan, Roberto Tateo, and Ara Sedrakyan

Phys. Rev. B **103**, L041302 — Published 13 January 2021

DOI: 10.1103/PhysRevB.103.L041302

Geometry of random potentials: Induction of 2D gravity in Quantum Hall plateau transitions

Riccardo Conti,[1] Hrant Topchyan,[2] Roberto Tateo,[3] and Ara Sedrakyan[2]

[1] *Grupo de Física Matemática da Universidade de Lisboa, Av. Prof. Gama Pinto 2, 1649-003 Lisboa, Portugal.*
[2] *Alikhanyan National Laboratory, Yerevan Physics Institute, Armenia*
[3] *Dipartimento di Fisica, Università di Torino, and INFN, Sezione di Torino, Via P. Giuria 1, I-10125 Torino, Italy*

(ΩDated: November 30, 2020)

Integer Quantum Hall plateau transitions are usually modeled by a system of non-interacting electrons moving in a random potential. The physics of the most relevant degrees of freedom, the edge states, is captured by a recently-proposed random network model, in which randomness is induced by a parameter-dependent modification of a regular network. In this paper we formulate a specific map from random potentials onto 2D discrete surfaces, which indicates that 2D gravity emerges in all quantum phase transitions characterized by the presence of edge states in a disordered environment. We also establish a connection between the parameter in the network model and the Fermi level in the random potential.

Introduction. The physics of plateau transitions in the Quantum Hall Effect (QHE) continues to be one of the most exciting research topic in modern condensed matter physics. Much of the current interest is motivated by the emergence of a similar type of physics in the context of topological insulators. The Quantum Hall plateau transition is in fact an example of a metal-insulator transition (see [1, 2] for a review) with the plateau region between the Landau Levels (LLs) corresponding to the insulating phase where all the bulk states are localized due to the external magnetic field. The transition is a disorder-induced localization/delocalization transition of Anderson type, characterized by a divergent localization length ξ with critical exponent ν.

Quantum Hall plateau transitions can be modelled by a system of non-interacting electrons moving in a 2D random potential (RP) $V(\mathbf{r})$, with $\mathbf{r} = (x, y)$, characterized by a white-noise Gaussian distribution. In the following, we shall consider RPs with a finite correlation length generated by Gaussian sources placed on a regular lattice, i.e.

$$V(\mathbf{r}) = \sum_{i,j} W_{i,j} \exp\left(-\frac{|\mathbf{r} - \mathbf{r}_{i,j}|^2}{2\sigma^2}\right) , \qquad (1)$$

where σ^2 is the variance, $\mathbf{r}_{i,j} = (i, j)$ is the position vector of the generic source and the coefficients $W_{i,j}$ are randomly chosen in $[-W, W]$, for some $W \in \mathbb{R}$. In such RP landscape, electrons with energy smaller than the Fermi level c are localized [3] due to the external magnetic field B and their state corresponds semi-classically to an orbital motion with small radius $R_L \sim 1/B$. They fill the Fermi sea, which actually consists of a collection of lakes with characteristic size l, as displayed in FIG. 1. At the boundary of a lake, the orbital motion of (edge) electrons combines with the reflection due to the potential giving rise to a precession motion along equipotential lines.

When an edge electron with energy $E > c$ approaches a saddle point, it may either tunnel through the potential barrier between the two neighbor lakes with probability

$$t^2 \sim \frac{1}{1 + e^{\varepsilon}} , \quad \varepsilon \propto (V - E) , \qquad (2)$$

or continue to move along the boundary of the same lake with probability $r^2 = 1 - t^2$ (see FIG. 2). The presence of such quantum scattering nodes at saddle points enables electrons to reach arbitrary distances with a finite probability and is at the origin of the localization/delocalization transition. Taking inspiration from this semi-classical picture, J. Chalker and P. Coddington (CC) [4] formulated a network model of quantum scattering nodes based on a regular lattice that is meant to provide an effective description of the physics of edge states.

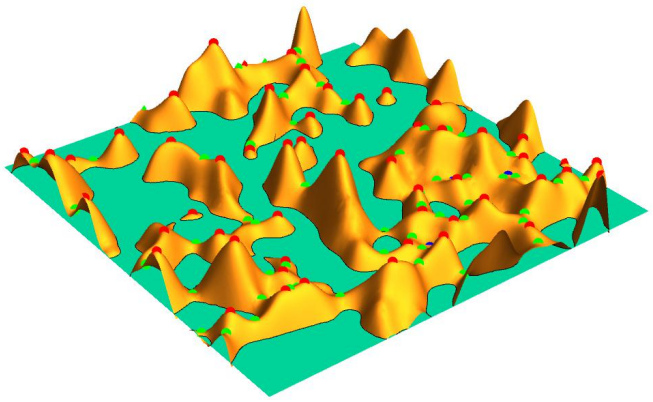


FIG. 1: RP generated by $N = 2500$ Gaussian sources ($W = 1$ and $\sigma = \sqrt{2}$) placed on a torus. Points mark maxima (red), minima (blue) and saddle points (green). The plane represents the Fermi level ($c = 0$).

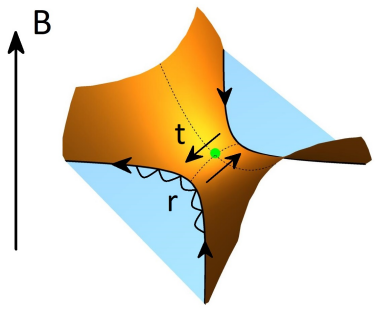


FIG. 2: Neighborhood of a saddle point (green dot) separating two lakes (blue areas) in a RP. The cycloid represents the motion of edge states along the boundary of a lake. The parameters r and t denote the reflection and transmission probabilities, respectively, while B is the magnetic field.

Its generalization on a Kagome lattice was proposed in [5] and a similar network model for the Spin Quantum Hall Effect (SQHE) was studied in [6, 7]. Numerical investigations of the localization length ξ around the critical point, i.e. $\xi \sim (t - t_{crit})^{-\nu}$ with $t_{crit} = 1/\sqrt{2}$, resulted in $\nu = 2.56 \pm 0.62$ for a regular lattice [8–10, 12, 13] and $\nu = 2.658 \pm 0.046$ for the Kagome lattice [5]. Both these values are not compatible with the experimental value $\nu = 2.38 \pm 0.06$ measured for plateau transitions in the integer QHE [14, 15]. A possible solution to fix the discrepancy was put forward in [16, 17] by considering random networks (RNs), which should better account for the disorder present in a RP. The numerical estimate obtained in this framework $\nu = 2.372 \pm 0.017$ [16, 17] confirms indeed a very good agreement with the experimental result. In fact, randomness generates – in the continuum limit – fluctuations of the background metric [16, 17], namely 2D quantum gravity, that are responsibile for the change of the critical exponents in network models, similarly to what was established by [18] in the context of minimal models of statistical mechanics. The primary objective of this paper is to show that 2D gravity is indeed emerging from the RPs framework, by establishing a precise correspondence between RNs and RPs. Notice that quantum gravity is also involved in the understanding of Fractional QHE [21, 22] revealing the physics of Laughlin wave-function. In that context, the interaction between fermions is responsible for the emergence of gravity in the bulk. Instead, in the present paper gravity is related to the 1+1 dimensional edge states, which originates from the RP.

Network models with geometric disorder. Let us briefly review the construction of RNs proposed in [16, 17]. Starting from a regular CC network, randomness is generated by making an extreme replacement, which consists in "opening" a scattering node in the horizontal (vertical) direction with probability p_0 (p_1) setting $t = 0$ ($t = 1$) (see FIG. 3), or leaving it unchanged with probability $1 - p_0 - p_1$. In the following, we shall set $p_n = p_0 = p_1$ to maintain statistical isotropy [16, 17]. In the RP picture, the scattering node represents a saddle point and the four squares surrounding it correspond to an alternate sequence of maxima and minima (see FIG. 3). After the extreme replacement, the scattering node becomes an hexagon containing a maximum (minimum) and two adjacent triangles both containing a minimum (maximum), as depicted in FIG. 3. Thus, starting from a regular network where all the faces are quadrangles and randomly making the extreme replacement with probability p_n, a polygonal tiling of the plane is obtained. In [17] it was shown that in this type of RNs the critical index ν has a non-trivial dependence on the replacement probability p_n, with a critical line for $p_n \in [0, 1/2]$. The best agreement with the experimental value of ν in the integer QHE is found for $(p_n, \nu(p_n)) = (1/3, 2.372 \pm 0.017)$.

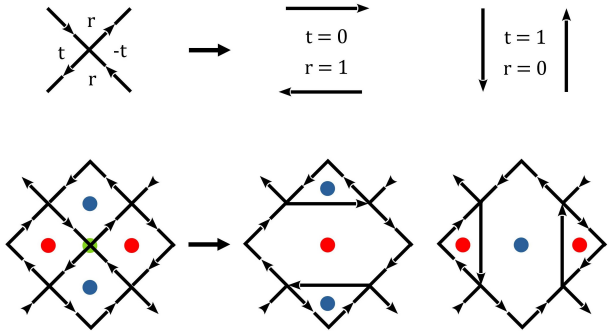


FIG. 3: Top: "opening" of a scattering node in the horizontal and vertical directions. Bottom: result of the extreme replacement on the network. Red, blue and green points mark maxima, minima and saddle points in the corresponding RP framework.

A natural question addressed in the present paper concerns the physical interpretation of the parameter p_n within the RP model.

Random potentials and discrete surfaces. The RP (1) corresponds to a 2D smooth surface characterized by N_{max} maxima, N_{min} minima, N_{sp} saddle points (see FIG. 1) and with Euler characteristics [23]

$$\chi = N_{min} + N_{max} - N_{sp} \, . \tag{3}$$

Connecting maxima and minima according to the gradient of $V(\mathbf{r})$ leads to a unique quadrangulation of the surface: a 2D discrete surface S made of $v = N_{max} + N_{min}$ vertices, e edges and $f = N_{sp}$ quadrangular faces (see FIG. 4). Denoting by n_i the connectivity of the $i-$th vertex, i.e. the number of edges connected to it, the Euler characteristics $\chi = v - e + f$ of S can be written as

$$2\pi\chi = \sum_{i=1}^{v} R(n_i) \, , \quad R(n) = \frac{\pi}{2}(4 - n) \, , \tag{4}$$

where, according to Gauss-Bonnet theorem, $R(n)$ can be interpreted as the discrete Gaussian curvature associated to each vertex of S. Equation (4) follows from $e = 2f = \frac{1}{2}\sum_{i=1}^{v} n_i$, which implies $\chi = v - e + f = v - f = \frac{1}{4}\sum_{i=1}^{v}(4 - n_i)$.
By construction, each face of S contains exactly one saddle point. Therefore, connecting saddle points belonging to nearest neighbor faces of S results in a dual 2D discrete surface S^*. The latter surface is made of $v^* = f$ vertices with connectivity 4, e^* edges and $f^* = v$ polygonal faces of size n, where n is the connectivity of the vertex of S lying within each face of S^* (see FIG. 4). By duality, each polygonal face of S^* carries a discrete Gaussian curvature $R(n)$ and brings a local contribution to $2\pi\chi$, as described by eq. (4). Hence, a RP is associated to a pair (S, S^*) of 2D discrete surfaces, which correspond to network models where the discrete Gaussian curvature of the surfaces is encoded either in the connectivity of the sites or in the number of sides of the polygons. In the following, the symbols S or S^* will stand for both the discrete surfaces and the corresponding networks.

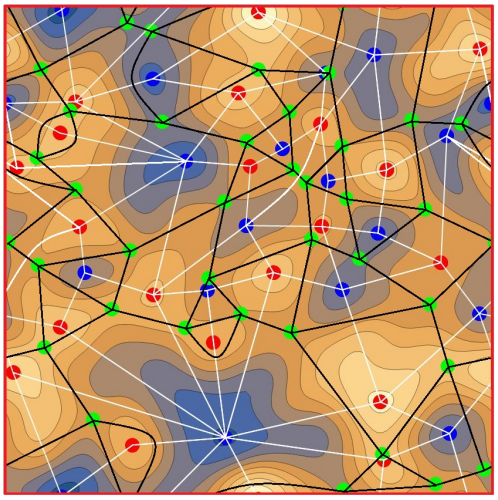


FIG. 4: Topography of a RP generated by $N = 900$ Gaussian sources ($W = 1$ and $\sigma = \sqrt{2}$) placed on a torus. Points mark maxima (red), minima (blue) and saddle points (green). White and black lines are the edges of S and S^*, respectively.

Random potentials vs. Random networks. The purpose of this section is to establish a correspondence between RPs and RNs in the case of a torus geometry. Consider a RP generated by $N = L^2$ Gaussian sources evenly distributed on a regular square lattice of size L with unit spacing and doubly periodic boundary conditions. Let $\mathbf{r}_{i,j} = (i \mod (L), j \mod (L))$ be the position vector of the generic source on the lattice. Then, the RP at the generic point $\mathbf{r} = (x, y) \in [1, L] \times [1, L]$ is

$$V(\mathbf{r}) = \sum_{i,j=1}^{L} \sum_{\mathbf{n}\in\mathbb{Z}^2} W_{i,j} \exp\left(-\frac{|\mathbf{r} - \mathbf{r}_{i,j} + \mathbf{n}L|^2}{2\sigma^2}\right), \quad (5)$$

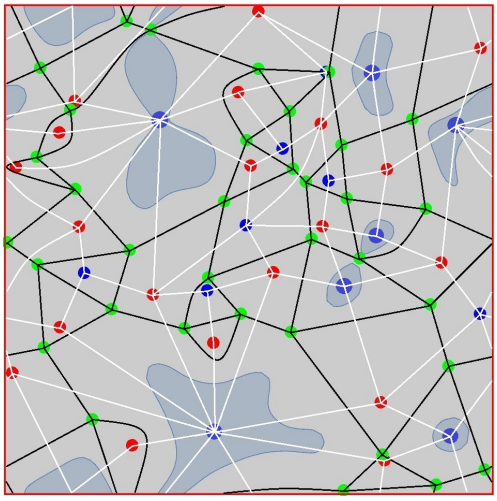


FIG. 5: Networks associated to the truncated discrete surfaces S_c and S_c^*, obtained from the RP displayed in FIG. 4 with $c = -1.2$. White and black lines are the links of S_c and S_c^*, respectively. The areas highlighted in light blue indicate the regions under the Fermi level.

where the range of the summation index $\mathbf{n} = (n_x, n_y)$ is restricted to $\{-1, 0, 1\} \times \{-1, 0, 1\}$ in the numerical simulation. Equation (3) implies that $N_{max} + N_{min} = N_{sp}$, since $\chi = 0$. In FIG. 6, the distributions of critical points per unit height h of the potential are reported. The statistical sample consists of $m = 45$ simulations with $L = 300$, $W = 1/10$ and $\sigma = \sqrt{2}$. Since at finite W and σ the potential $V(\mathbf{r})$ is bounded, these distributions are defined on a finite support, also in the limit $L \to \infty$. However, in the case under consideration, they are well approximated by Gaussian distributions with expectation values $\mu_{max} = -\mu_{min} = 0.187$, $\mu_{sp} = 0$ and standard deviations $\sigma_{max} = \sigma_{min} = \sigma_{sp} = 0.119$. Following the procedure described in the previous section,

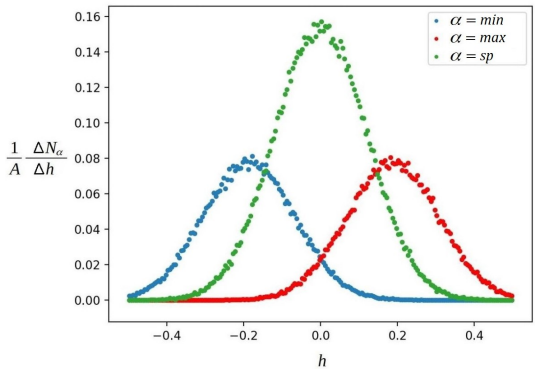


FIG. 6: Number of maxima (ΔN_{max}), minima (ΔN_{min}) and saddle points (ΔN_{sp}) in the height range $[h, h + \Delta h]$, with $\Delta h = 1/200$, divided by the area A of the lattice. The statistical sample consists of $m = 45$ simulations with $L = 300$, i.e. $A = mL^2$, $W = 1/10$ and $\sigma = \sqrt{2}$.

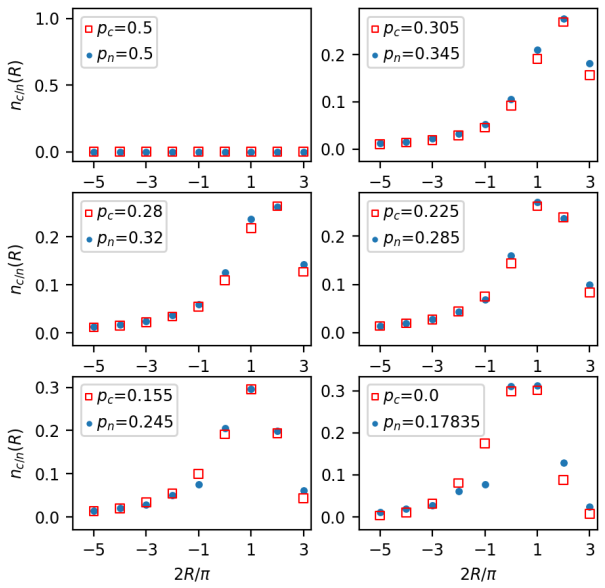


FIG. 7: Curvature distributions for the RN (blue dots) and the dual network S_c^* (red squares) for various values of the parameters p_n and p_c which minimize the SSE.

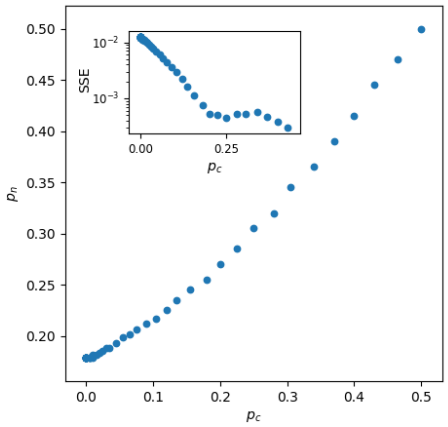


FIG. 8: Correspondence between the replacement probability p_n and p_c obtained searching for the best match between the two curvature distributions. The inset plot gives the estimated SSE as a function of p_c in logarithmic scale.

a discrete surface S or equivalently S^* can be uniquely associated to the RP (see FIG. 4). The introduction of a Fermi level c produces a truncated surface S_c in which the vertices lying below c and belonging to the same lake are replaced with a single vertex, as displayed in FIG. 5. This operation is indeed physically meaningful since the scattering of edge states is not affected by bulk electrons. Therefore, a change in the Fermi level induces a flow within the space of discrete surfaces parametrized by c.

The removal of sites due to the truncation generates polygonal faces in S_c^* with different sizes compared to those of S^* (see FIG. 5). The net effect of this procedure is reminiscent of that induced in the CC network by the surgery defined in [16, 17] and leading to RNs. For this reason, we expect the replacement probability p_n of RNs to be somehow related to the Fermi level in RPs. However, for the purpose of comparing these two models, it is first necessary to restore the particle-hole duality in the RP framework because the RNs, which are described in the continuum limit by a Dirac fermion theory [20], possess it. To this aim, the range of energies accessible to an edge fermion in the RP should be restricted from $[c, +\infty]$ to the symmetric interval $I_c = [-|c|, |c|]$. We shall refer to the complementary interval $\bar{I}_c = [-\infty, -|c|] \cup [|c|, +\infty]$ as the *non-valid region*. Next, notice that the replacement probability p_n is equivalent – at large network size – to half the ratio of the number of removed scattering nodes to the total number of nodes. Therefore, the quantity

$$p_c = \frac{1}{2} \frac{\#\,\text{saddle points} \in \bar{I}_c}{\#\,\text{saddle points} \in (I_c \cup \bar{I}_c)} \,, \qquad (6)$$

appears to be the most appropriate parameter of the RP to be put in relation to p_n. Since the distribution of saddle points per unit height h is approximately Gaussian (see FIG. 6), the parameter p_c can be related to the Fermi level via the complementary error function, $p_c \simeq \frac{1}{2}\mathbf{erfc}\left(|c|/(\sqrt{2}\sigma_{sp})\right)$.

To find the relation between p_n and p_c, we consider the distribution of discrete Gaussian curvatures R of the polygons tiling both the RN and the dual network S_c^* for several values of p_n and p_c, respectively. The criterion adopted for the association between p_n and p_c is the minimization of the sum of squared errors,

$$SSE = \sum_{m \geq 1} \left(n_n(R(m)) - n_c(R(m))\right)^2 \,, \qquad (7)$$

where $n_n(R)$ and $n_c(R)$ denote the number of polygons with curvature R divided by the total number of polygons in the RN and in S_c^*, respectively, with $R(m)$ as in eq. (4). In FIG. 7, curvature distributions in both the RN and S_c^* are compared for some values of p_n and p_c that minimize the SSE. The statistical samples consist of more than 50 RN simulations on a 100×1000 network for each value of $p_n \in [0, 1/2]$ and 45 RP simulations on a square lattice of size $L = 300$ for each value of $c \in [0, 1/2]$. A good agreement between the two models is obtained for a suitable correspondence $p_n \leftrightarrow p_c$, as reported in FIG. 8. We see that for $p_c \gtrsim 0.35$ the relation $p_n(p_c)$ is approximately $p_n = p_c$, while for smaller values of p_c the curve is deviating from the linear behavior ending at $p_n(0) \simeq 0.178$. The origin of this deviation is related to the fact that $p_n = 0$ corresponds to a regular network which can be associated to a periodic potential, while the RP is intrinsically disordered for any value of p_c. Periodic potentials have zero measure in the space of all RPs, therefore it is not surprising that the distribution of curvatures in the RN is less sensitive to variations of p_n

around $p_n = 0$. Similar considerations might also justify the discrepancy between $n_n(R)$ and $n_c(R)$ that can be observed in the bottom right plot of FIG. 7. We shall leave a more systematic study of this issue to the future.

Conclusions. There are strong evidences that the field-theory description of plateau transitions corresponds to a model of fermions interacting with random gauge and scalar potentials and also with structurally-disordered geometry. Indicating that, in the scaling limit, localization transitions of this type are correctly described by matter fields coupled to 2D quantum gravity. Starting from a random potential model, we have explicitly constructed a map onto the 2D disordered graphs S_c and S_c^* depending on the Fermi-level. Thus, observing the appearance of the basic ingredient of random network models [16, 17] for Quantum Hall plateau transitions and giving an interpretation of the replacement probability in term of the Fermi energy. S_c and S_c^*, being quadrangular and polygonal tilings of the plane, have a straightforward interpretation as discrete random surfaces, explicitly showing the emergence of 2D gravity. As discussed also in [16], the notion of functional measure of random surfaces remains an open problem. From the current analysis, it appears that the distribution of Gaussian curvatures on the random surface associated with the random potential coincides with the corresponding distribution in the random network model, suggesting that the functional measure of random surfaces can be defined in terms of the measure of random potentials. In conclusion, we revealed a deep link between random potentials in Anderson localization problem and 2D curved surfaces, where the edge states responsible for plateau transitions live.

Acknowledgments. A.S. acknowledge University of Turin and INFN for hospitality and ARC grant 18T-1C153 for financial support. This work was also partially supported by the INFN project SFT and by the FCT Project PTDC/MAT-PUR/30234/2017 "Irregular connections on algebraic curves and Quantum Field Theory". R.C. is supported by the FCT Investigator grant IF/00069/2015 "A mathematical framework for the ODE/IM correspondence".

[1] B. Huckestein, Rev. Mod. Phys. 67, 357 (1995).
[2] B. Kramer, T. Ohtsuki and S. Kettemann Phys. Rep. 417, 211 (2005).
[3] E. Abrahams, P. W. Anderson, D. C. Licciardello, and T. V. Ramakrishnan, Phys. Rev. Lett. 42, 673 (1979).
[4] J. T. Chalker and P. D. Coddington, J. Phys. C 21, 2665 (1988).
[5] N. Charles, I. Gruzberg, A. Klümper, W. Nudding, and A. Sedrakyan, ArXiv:2003.08167.
[6] V. Kagalovsky, B. Horovitz, Y. Avishai, and J. T. Chalker, Phys. Rev. Lett. 82, 3516 (1999).
[7] I. A. Gruzberg, A. W. W. Ludwig, and N. Read, Phys. Rev. Lett.82, 4524 (1999).
[8] K. Slevin and T. Ohtsuki, Phys. Rev. B 80, 041304(R) (2009).
[9] M. Amado, A. V. Malyshev, A. Sedrakyan, and F. Domínguez- Adame, Phys. Rev. Lett. 107, 066402 (2011).
[10] H. Obuse, I. A. Gruzberg, and F. Evers, Phys. Rev. Lett. 109, 206804 (2012).
[11] K. Slevin and T. Ohtsuki, Int. J. Mod. Phys. Conf. Ser. 11, 60 (2012).
[12] W. Nuding, A. Klümper, and A. Sedrakyan, Phys. Rev. B 91, 115107 (2015).
[13] J. P. Dahlhaus, J. M. Edge, J. Tworzydło, and C. W. J.Beenakker, Phys. Rev. B 84, 115133 (2011).
[14] W. Li, G. A. Csăthy, D. C. Tsui, L. N. Pfeiffer, and K. W. West, Phys. Rev. Lett. 94, 206807 (2005).
[15] W. Li, C. L. Vicente, J. S. Xia, W. Pan, D. C. Tsui, L. N. Pfeiffer, and K. W. West, Phys. Rev. Lett. 102, 216801 (2009).
[16] I. A. Gruzberg, A. Klümper, W. Nuding, and A. Sedrakyan, Phys. Rev. B, 95, 125414 (2017).
[17] A. Klümper, W. Nuding, and A. Sedrakyan, Phys. Rev. B 100, 140201(R) (2019).
[18] V. G. Knizhnik, A. M. Polyakov, and A. B. Zamolodchikov, Mod. Phys. Lett. A 03, 819 (1988).
[19] H.A. Fertig and B.I. Halperin, Phys. Rev. 36, 7969 (1987).
[20] A. Sedrakyan, Continuum limit of Chalker and Coddington network model, Talk at Bremen conference, July, 2008.
[21] F. D.M. Haldane, Phys.Rev.Lett.107, 116801 (2011).
[22] T. Can, M. Laskin, P. B. Wiegmann, Annals of Physics 362 (2015) 752–794.
[23] J. Milnor, Morse Theory-Princeton University Press, Pinceton, New Jersey 1963.